Inorganic Chemistry

ARTICLE

pubs.acs.org/IC

Remote Effects of Axial Ligand Substitution in Heterometallic Cr≡Cr···M Chains

Michael Nippe, Yevgeniya Turov, and John F. Berry*

Department of Chemistry, University of Wisconsin—Madison, 1101 University Avenue, Madison, Wisconsin 53706, United States

Supporting Information

ABSTRACT: The heterometallic complexes $CrCrM(dpa)_4Cl_2$ (dpa = 2,2′-dipyridylamide) featuring linear Cl−Cr≡Cr···M−Cl chains can regiospecifically be modified via axial ligand substitution to yield OTf−Cr≡Cr···M−Cl chains (OTf = triflate) with M being Fe, Mn, or Co. The effect of OTf substitution on the Cr side of the molecule has an unusual and profound structural impact on the square-pyramidal transition metal M. Specifically, elongation of the four equatorial M−N_{py} bonds and the axial M−Cl bonds by 0.03 and 0.09 Å for Fe and 0.07 and 0.11 Å for Mn is observed. The longer M−Cl and M−N_{py} bonds result from subtle interactions between the equatorial dpa ligand and the three metal ions. The equatorial dpa ligand responds to the introduction of the more labile OTf ligand at Cr by binding more strongly to this Cr ion which in turn weakens bonding to M. The ligand field experienced by M can be tuned by changing the Cr axial ligand, and this effect is observed in electrochemical measurements of the iron compounds.

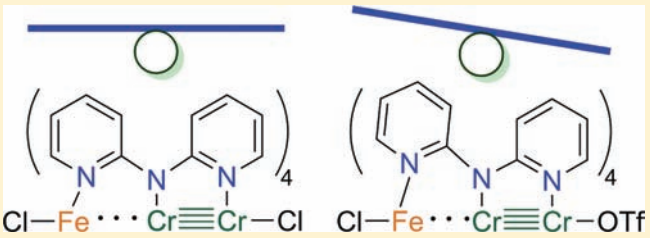

INTRODUCTION

The reactivity of heterometallic coordination complexes has recently been of interest,[1,2] especially with respect to models of heterometallic enzyme active sites.[3] In this respect, the differential reactivity of M−L vs M′−L bonds in heterometallic molecules containing both M and M′ deserves inquiry. Research efforts in our lab have afforded rational synthetic methods to access a class of heterometallic complexes $CrCrM(dpa)_4Cl_2$ that contain linear Cl−Cr≡Cr···M−Cl chains, with M = Mn(II),[4] Fe(II),[5] Co(II),[6] or Zn(II),[7] (here, dpa = the anion of 2,2′-dipyridylamine). The metal atoms are ligated equatorially by the nitrogen atoms of dpa and the outer metal atoms are ligated axially by chloride. These linear frameworks are ideally suited to allow for experiments probing the nature of secondary interactions at the N_4MCl square pyramidal transition metal center in response to differing axial ligands appended to the Cr≡Cr multiply bonded group (Scheme 1). Whether a specific change made at the Cr end of the molecule has any effect on the geometry of M may have important implications for the nature of charge distribution and Cr···M interactions in these molecules.

We report herein the preparation of new mixed chloride/triflate compounds and the novel ditriflate compound $CrCrFe(dpa)_4(OTf)_2$ (OTf = $^{-}OSO_2CF_3$) along with crystallographic, spectroscopic, and electrochemical data. These data provide evidence that the geometry and properties of M are strongly influenced by ligand substitution on the Cr side of the linear framework. This *remote influence* is induced by a tilting of the dpa ligands about their central amido nitrogen atoms in response to the variable ligand field strength at the terminal Cr atom.

EXPERIMENTAL SECTION

Materials and Methods. All reactions were carried out under a dry N_2 atmosphere using Schlenk techniques and glovebox methods. Solvents diethyl ether (Et_2O), acetonitrile (CH_3CN), and hexanes were purified using a Vacuum Atmospheres solvent purification system. Dichloromethane was freshly distilled under an N_2 atmosphere over CaH_2 prior to use. $Fe(OTf)_2$ (Wako) and Tl(OTf) (Strem) were purchased and used as received. NaSCN (Sigma-Aldrich) was dried at 80 °C for ∼10 h under dynamic vacuum prior to use. The ligand dpaH (2,2′-dipyridylamine, Sigma-Aldrich) was recrystallized from hot hexanes prior to use. $Cr_2(dpa)_4$,[5] $CrCrFe(dpa)_4Cl_2$ (**1**),[5] $CrCrMn(dpa)_4Cl_2$ (**2**),[4] and $CrCrCo(dpa)_4Cl_2$ (**7**)[6] were prepared according to literature procedures. Cyclic voltammograms (CVs) were taken on a BAS Epsilon-EC instrument using CH_2Cl_2 solutions with 0.1 M NBu_4PF_6 and <1 mM substrate. The electrodes were as follows: glassy carbon (working), Pt wire (auxiliary), and Ag/Ag^+ in CH_3CN (reference). The potentials were referenced versus the ferrocene/ferrocenium redox couple, by externally added ferrocene. Elemental analysis was carried out by Columbia Analytical Services in Arizona, USA and Midwest Microlab, LLC in Indiana, USA. X-Band EPR spectra of frozen solutions (CH_2Cl_2) of **8**/**8-iso** were recorded at 4 and 8 K temperature using a Bruker EleXsys EPR spectrometer: E-500-A console with ER 049SX SuperX Bridge and SuperX Cavity. The sample temperature was set using an Oxford Instruments ESR 900 continuous-flow liquid helium cryostat regulated by an Oxford ITC4 temperature controller. The IR spectra were taken on a Bruker Tensor 27 using KBr techniques. ^1H NMR spectra were recorded on a Varian INOVA-500 spectrometer. The

Received: April 5, 2011
Published: September 20, 2011

Scheme 1

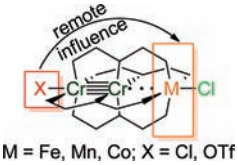

magnetic susceptibilities of compounds **3** and **5** were established using an Evans balance, with proper diamagnetic corrections calculated from Pascal's constants.[8]

X-ray Structure Determinations. Crystallographic data were measured at the Molecular Structure Laboratory of the Chemistry Department of the University of Wisconsin—Madison. Crystals were selected under oil under ambient conditions. Block-shaped single crystals were attached to the tip of a MiTeGen MicroMount. The crystals were mounted in a stream of cold nitrogen at 100(1) K and centered in the X-ray beam using a video monitoring system. The crystal evaluation and data collection were performed on a Bruker Quazar SMART APEX-II diffractometer with Mo Kα (λ = 0.71073 Å) radiation. The data were collected using a routine to survey reciprocal space, and were indexed by the SMART program.[9] The structures were solved using direct methods and refined by least-squares refinement on F^2 followed by difference Fourier synthesis.[10] All hydrogen atoms were included in the final structure factor calculation at idealized positions and were allowed to ride on the neighboring atoms with relative isotropic displacement coefficients.

The crystal structure of **5** deserves additional comments: The structure was solved with space group *C*2/*c*, but was found to refine poorly. However, the model refines well in the space group *Cc* as an inversion twin with a minor component contribution of 19%. The two independent molecules were solved using the program smtbx with charge flipping and refined over several cycles to complete the ligands.[11] One of the four independent triflate ligands is disordered (18%/82%), as are the Cr and Fe atoms. The metal atoms (Fe and Cr) were not refined anisotropically except Cr2/Cr2A and Cr4/Cr4A, which were sufficiently far apart that anisotropic refinement was appropriate. The metal atoms had variable occupancy of 76%/24% ratio in one molecule and 43%/57% ratio in the second molecule. The disordered triflate ions were also not refined anisotropically, except for O7, S4, and S4A atoms. There is also one partially occupied disordered tetrahydrofuran molecule in the asymmetric unit, which was not refined anisotropically.

OTfCrCrFeCl(dpa)$_4$ (3). *Route A.* A suspension of TlOTf (66 mg, 0.188 mmol) in CH_2Cl_2 (8 mL) was slowly added to a stirred solution of **1** (185 mg, 0.188 mmol) in CH_2Cl_2 (25 mL) at 0 °C. The mixture was stirred for a minimum of 1 h during which it was allowed to warm to room temperature. Filtration through Celite and subsequent diffusion of hexanes into the yellow−brown solution yielded crystalline material of **3**. Yield: 120 mg, 62%. Anal. Calcd. for $C_{41}H_{32}ClFeCr_2F_3N_{12}O_3S$ (**3**): C 48.04%, H 3.15%, N 16.40%; found C 47.64%, H 3.31%, N 16.05%. μ_{eff} (298 K, μ_B) = 4.37. ^{1}H NMR (CD_2Cl_2, 500 MHz, ppm): δ 112.36, 70.66, 40.49, 6.39, 4.30, 4.09, 3.64, −1.97. IR (KBr, cm^{-1}): 1605 m, 1595 m, 1560 w, 1549 w, 1469 s, 1424 s, 1367 s, 1310 m, 1285 m, 1235 m, 1217 m, 1167 m, 1153 m, 1109 w, 1051 w, 1027 m, 1018 m, 920 w, 880 m, 860 w, 764 s, 740 m, 648 w, 634 m, 570 w, 517 m.

Route B. CH_2Cl_2 (30 mL) was added to a solid mixture of **1** (64 mg, 0.07 mmol) and **5** (80 mg, 0.07 mmol) and the resulting yellow−brown solution was stirred for a minimum of 2 h at room temperature. Subsequent filtration and diffusion of hexanes into the CH_2Cl_2 solution yielded crystalline material of **3**, in very high purity as determined by ^{1}H NMR spectroscopy. Yield: 90 mg, 63%.

OTfCrCrMnCl(dpa)$_4$ (4). Compound **4** was prepared from **2** analogously to *Route A* for the preparation of **3**. Yield: 30 mg, 53%. Anal. Calcd. for $C_{46.2}H_{43.8}Cl_3Cr_2F_3MnN_{12}O_3S$ (**4**·**2CH$_2$Cl$_2$**): C, 43.25%; H, 3.04%; N, 14.08%. Found: C, 42.90%; H, 3.38%; N, 13.71%. IR (KBr, cm^{-1}): 1606 s, 1595 s, 1560 w, 1550 w, 1470 s, 1459 s, 1424 s, 1366 m, 1310 m, 1287 w, 1235 m, 1217 m, 1167 m, 1153 m, 1106 w, 1028 m, 1018 m, 1007 w, 920 w, 879 w, 860 w, 764 m, 748 w, 741 m, 668 w, 649 w, 635 m, 538 w, 517 w.

CrCrFe(dpa)$_4$(OTf)$_2$ (5). THF (35 mL) was added to a solid mixture of orange $Cr_2(dpa)_4$ (380 mg, 0.48 mmol) and off-white $Fe(OTf)_2$ (190 mg, 0.53 mmol). The suspension was heated to reflux while stirring for a minimum of 7 h, after which the formation of a lustrous gold precipitate was observed. The crude product was isolated by filtration. X-ray quality crystals were grown by diffusion of hexanes into a solution of the compound in dichloromethane. Yield: 410 mg, 74%. Anal. Calcd. for $C_{43.5}H_{35}Cr_2F_6FeN_{12}O_6S_2Cl_3$ (**5**·0.5CH_2Cl_2·0.15C_4H_8O): C, 42.92%; H, 2.95%; N, 13.90%. Found: C, 43.43%; H, 2.89%; N, 14.10%. μ_{eff} (298 K, μ_B) = 4.78. ^{1}H NMR (CD_2Cl_2, 500 MHz, ppm): δ 105.02, 71.23, 39.29, 4.49, 3.84, 2.47, −0.76, −2.65. IR (KBr, cm^{-1}): 1607 m, 1598 m, 1551 w, 1471 s, 1430, 1365 m, 1314 m, 1287 m, 1235 m, 1213 m, 1155 m, 1028 m, 1018 m, 881 w, 861 w, 766 m, 740 w, 636 m.

(SCN)CrCrFeCl(dpa)$_4$ (6). Compound **3** was formed in situ via route A, from **1** (140 mg, 0.14 mmol) and TlOTf (50 mg, 0.14 mmol). A solution (3.7 mL) of NaSCN (38 mM) was added dropwise over 4 min to the yellow−brown solution of **3** and a slight color change to red−brown was observed. Solvent was removed under reduced pressure, yielding a red−brown microcrystalline solid. The solid was washed with 10 mL of Et_2O and extracted into 20 mL of CH_2Cl_2. Solvent diffusion of Et_2O into the solution mixture yielded a small amount of crystalline material. Yield: 6.4 mg, 5%. Anal. Calcd. for $C_{41.5}H_{33}Cl_2FeCr_2F_3N_{13}S$ (**6**·0.5CH_2Cl_2): C 51.03%, H 3.38%, N 18.65%; found C 51.39%, H 3.60%, N 18.34%. IR (KBr, cm^{-1}): 2040 s, 1605 m, 1595 m, 1548 w, 1466 s, 1426 s, 1369 m, 1311 m, 1282 w, 1154 m, 1017 m, 880 w, 859 w, 764 m, 739 m, 647 w, 538 w, 518 w.

OTfCrCrCoCl(dpa)$_4$/ClCrCrCoOTf(dpa)$_4$ (8/8-iso). Compounds **8**/**8-iso** were prepared as a mixture from **7** analogously to *Route A* for the preparation of **3**. Yield: 70 mg, 42% Anal. Calcd. for $C_{41}H_{32}ClCoCr_2F_3N_{12}O_3S$ (**8**/**8-iso**): C 47.89%, H 3.14%, N 16.35%; found C 47.37%, H 2.96%, N 15.73%. IR (KBr, cm^{-1}): 3070 w, 3031 w, 2972 w, 2853 w, 1607 s, 1596 s, 1550 w, 1469 s, 1429 s, 1371 s, 1313 s, 1286 s, 1234 s, 1213 s, 1155 s, 1112 w, 1018 s, 881 m, 861 m, 765 s, 740 s.

RESULTS AND DISCUSSION

Synthesis. The synthetic methods and numbering for the compounds reported here are outlined in Scheme 2. Reaction of **1** with one equivalent of thallium triflate (TlOTf) in CH_2Cl_2 at 0 °C results in the regiospecific substitution of the Cr-bound chloride (Cl_{Cr}) ion for triflate, yielding the monotriflate complex **3** in good yield (63%) and TlCl as a precipitate (eq 1, Scheme 2). The regioselectivity of the reaction and the characterization of the product as a single component was established via ^{1}H NMR spectroscopy and X-ray crystallography (*vide infra*). The selectivity of this reaction is likely promoted by the kinetic lability of Cl_{Cr} (d(Cr−Cl) = ~2.7 Å) as compared to Cl_{Fe} (d(Fe−Cl) = ~2.3 Å) and the possible thermodynamic preference of the Cr_2 unit for the weaker axial σ donor OTf ligand in **3** vs Cl. The same kinetic argument holds for the corresponding reaction of **2** with TlOTf to generate **4**, because of the large difference in bond distances for the metal-chloride bonds in **2**,[4] d(Cr−Cl) = ~2.7 Å as compared to d(Mn−Cl) = ~2.3 Å. Alternatively, **3** can be furnished in high purity via reaction of **1** with the ditriflate compound **5** (eq 2). This equilibration reaction is the preferred synthetic route to **3** because it avoids the use of thallium salts and can easily be scaled up.

dx.doi.org/10.1021/ic2011309 |*Inorg. Chem.* 2011, 50, 10592–10599

Compound **5** is conveniently prepared in analogy to the dichloride compound **1** by metalation of $Cr_2(dpa)_4$ with ferrous ditriflate ($Fe(OTf)_2$) in tetrahydrofuran (THF) at elevated temperatures. The resulting solid material can be extracted with CH_2Cl_2 and crystallizes upon addition of hexanes. X-ray crystallographic examination of the crystalline sample is consistent with the molecular connectivity of **5** as drawn in Scheme 2 (*vide infra*).

Scheme 2

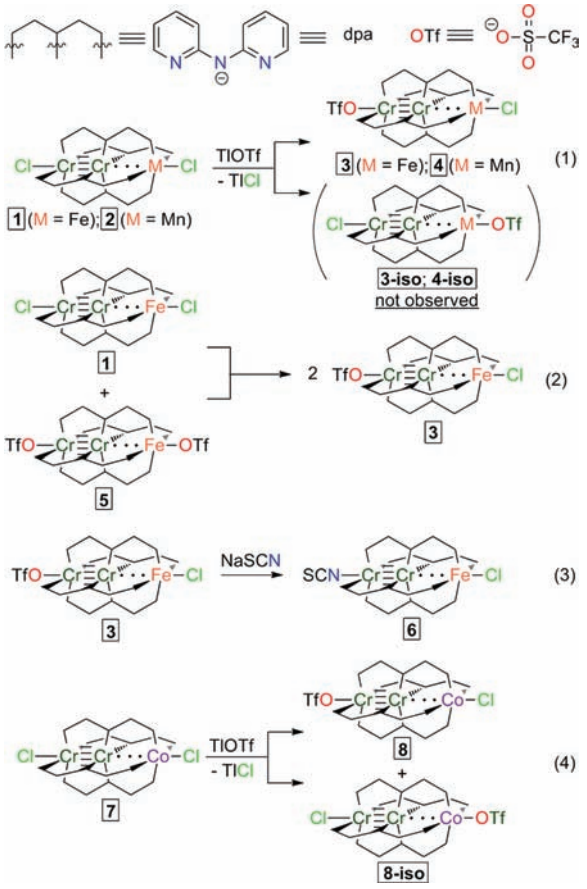

The ability of compound **3** to serve as a synthon for the selective generation of further heteroligated X−Cr≡Cr···Fe−Cl compounds was established by preparation of **6** (eq 3): careful addition of one equivalent of a dilute solution of sodium thiocyanate (NaNCS) in acetonitrile (CH_3CN) to a CH_2Cl_2 solution of **3** results in substitution of the labile OTf^- ligand by NCS^- to furnish the isothiocyanato complex **6**. The yield of this reaction is poor due to a side reaction including Fe demetalation; thus, reliable synthetic routes to heteroligated species still need to be found. Nevertheless, good quality single crystals of **6** were obtained via diffusion of Et_2O into CH_2Cl_2.

We also investigated the possibility of extending the initial synthetic protocol of generating **3** via Cl^- abstraction from **1** (using TlOTf) to structural analogs of **1**, namely $CrCrMn(dpa)_4Cl_2$, **2**, and $CrCrCo(dpa)_4Cl_2$, **7**. Like **1**, compound **2** undergoes regiospecific ligand exchange at the Cr end of the molecule with TlOTf furnishing **4** as the sole product (eq 1). In the case of **7**, however, no such selectivity can be reported, and it is of interest to note that in the low-spin form, the Co−Cl and Cr−Cl bond distances are equal (d(Co−Cl) = ∼2.6 Å and d(Cr−Cl) = ∼2.6 Å), whereas the high-spin form of **7** resembles **1** and **2** with d(Co−Cl) = ∼2.4 Å and d(Cr−Cl) = ∼2.6 Å.[6] A product mixture containing the monotriflate compounds **8** and **8-iso** was obtained (eq 4) with OTf^- bound to either the terminal Cr or the Co ion, respectively. To our knowledge, this is the first report of two compounds that are heterometallic and heteroligated isomers. We have not been able to separate these isomers.

Crystal Structures. X-ray crystallographic results are presented in three parts: (1) a general discussion addresses metal atom disorder and intermolecular interactions between the trinuclear compounds and cocrystallized solvent molecules where applicable; (2) a detailed discussion addresses the assignment of the noncentrosymmetric space group *Cc* to structures of **3**, **4**, **5**, and **8**/**8-iso**; (3) a detailed discussion of structural changes induced by ligand substitution is given. Crystallographic details and bond distances for all discussed compounds are given in Tables 1 and 2, respectively.

1. General Discussion. Single-crystalline material of compounds **3**, **4**, and **8**/**8-iso** was obtained from CH_2Cl_2/hexanes

Table 1. Crystallographic Data

	100 K				
compound	**3**	**4**	**5**	**6**	**8/8-iso**
formula	$Cr_2Fe(C_{10}H_8N_3)_4(CF_3SO_3)Cl\cdot 2CH_2Cl_2$	$Cr_2Mn(C_{10}H_8N_3)_4(CF_3SO_3)Cl\cdot 2CH_2Cl_2$	$[Cr_2Fe(C_{10}H_8N_3)_4(CF_3SO_3)_2]_2\cdot CH_2Cl_2\cdot 0.3C_4H_8O$	$Cr_2Fe(C_{10}H_8N_3)_4(NCS)Cl\cdot Et_2O$	$Cr_2Co(C_{10}H_8N_3)_4(CF_3SO_3)Cl\cdot 2CH_2Cl_2$
crystal system	monoclinic	monoclinic	monoclinic	monoclinic	monoclinic
space group	*Cc*	*Cc*	*Cc*	$P2_1/c$	*Cc*
a, Å	18.961(2)	18.981(2)	34.4912(9)	16.3144(5)	18.861(2)
b, Å	16.951(2)	16.917(2)	17.8894 (5)	16.1054(5)	16.999(2)
c, Å	15.607(1)	15.641(1)	16.8300(4)	17.5820(5)	15.574(2)
β, °	109.088(1)	108.931(1)	108.302(1)	103.998(2)	109.330(2)
V, Å^3	4740.3(7)	4750.8(7)	9859.3(4)	4482.5(2)	4712.0(9)
Z	4	4	8	4	4
ρ, Mg m^{-3}	1.674	1.669	1.593	1.494	1.689
R1[a], wR2[b] ($I > 2\sigma(I)$)	0.0388, 0.1012	0.0315, 0.0791	0.0467, 0.1312	0.0531, 0.1414	0.0500, 0.1224
R1[a], wR2[b] (all data)	0.0511, 0.1168	0.0374, 0.0891	0.0484, 0.1323	0.0541, 0.1422	0.0563, 0.1274

[a] $R1 = 3||F_o| - |F_c||/3|F_o|$. [b] $wR2 = [3[w(F_o^2 - F_c^2)^2]/3[w(F_o^2)^2]]^{1/2}$, $w = 1/\sigma 2(F_o^2) + (aP)2 + bP$, where $P = [\max(0 \text{ or } F_o^2) + 2(F_c^2)]/3$.

dx.doi.org/10.1021/ic2011309 |*Inorg. Chem.* 2011, 50, 10592–10599

Table 2. Selected Bond Distances in 1 ($1\cdot CH_2Cl_2$, 100 K), 2, 3, 4, 6, and 8/8-iso

compound	M−Cl, Å	M−N_{avg}, Å	M···Cr, Å	Cr≡Cr, Å	Cr_{inner}−N_{avg}, Å	Cr_{outer}−N_{avg}, Å	δ, Å
1 (M = Fe)	2.300(2)	2.157[4]	2.715(2)	2.025(2)	2.028[2]	2.119[5]	0.038(5)
2 (M = Mn)	2.259(2)	2.190[1]	2.781(1)	2.040(1)	2.03[2]	2.130[5]	0.060(3)
3 (M = Fe)	2.3966(9)	2.190[3]	2.7317(7)	1.9641(7)	2.029[3]	2.077[3]	0.113(3)
4 (M = Mn)	2.3707(8)	2.262[3]	2.8528(6)	1.9573(6)	2.036[2]	2.076[3]	0.186(3)
6 (M = Fe)	2.354(1)	2.173[3]	2.6957(7)	2.0187(8)	2.034[3]	2.110[3]	0.063(3)
8 (M = Co)	2.3595(17)	2.161[5]	2.7152(17)	1.939(3)	2.019[3]	2.032[6]	0.129(6)
8-iso (M = Co)	2.641(6)	2.034[10]	2.543(7)	1.964(6)	2.030[4]	2.141[11]	−0.107(11)

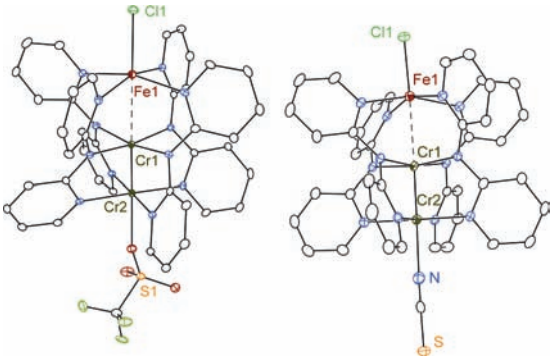

Figure 1. Molecular structures of **3** (left) and **6** (right) with displacement ellipsoids drawn at the 30% probability level. Hydrogen atoms have been omitted for clarity.

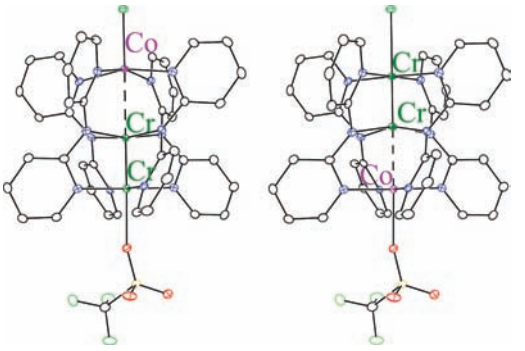

Figure 2. Molecular structures of cocrystallized **8** (left) and **8-iso** (right) with displacement ellipsoids drawn at the 30% probability level. Hydrogen atoms have been omitted for clarity.

solvent mixtures. The molecules crystallize as $M\cdot 2CH_2Cl_2$ solvates in the monoclinic space group *Cc*. Because Cr and Fe (or Mn or Co) are crystallographically indistinguishable, the assignments of metal atom identities are based on expected distances for quadruply bonded Cr≡Cr units. The metal atoms in **3** (Figure 1, left) and **4** show no sign of metal atom disorder in contrast to their precursors **1** and **2**, respectively. The absence of disorder of the metal atom positions indicates that the crystals considered contain solely **3** (or **4**) and none of the possible structural isomer **3-iso** (or **4-iso**), because cocrystallization of the product mixture would be expected as in the case of **8**/**8-iso**; however, it is possible that isomers of **3-iso** and **4-iso** do form in the reaction and were simply not seen in the particular crystals that were examined crystallographically. But, ^{1}H NMR studies on **3** show the existence of only one species in solution of the bulk sample, and we may therefore discount the possibility that **3-iso** is formed. In the case of **8-iso**, both the high-spin and low-spin forms of **7** are present in solution and the low-spin case has elongated Co−Cl bond distances which results in the formation of **8-iso**. Conversely, compounds **1** and **2** are present solely in the high-spin form in which the Cr−Cl bond is longer than the M-Cl bond and the formation of **3-iso** and **4-iso** is not probable.

Cocrystallization of isomers is observed for the product mixture after reaction of **7** with TlOTf: the metal atoms in **8**/**8-iso** are clearly disordered with relative occupancies of 67%/33%, respectively, indicating cocrystallization of the two distinguished molecular entities, featuring either an N_4CoCl (in **8**) or N_4CoOTf (in **8-iso**) unit (Figure 2).

Another important feature of the crystal structures of **3**, **4**, and **8** is the proximity of a solvent CH_2Cl_2 molecule (d(Cl···H(CH_2Cl_2) = 2.65 Å) to the chloro ligand at a distance less than the sum of their van der Waals radii (Figure 3), which is indicative of an intermolecular interaction (directional Cl···H−C angle = 152°). Similar interactions in crystalline material of **1** and **2** have recently been shown to have a significant influence on the spectroscopic properties of the paramagnetic metal.[4]

Compound **6** (Figure 1, right) was crystallized as **6**·Et_2O. The metal atoms are not disordered indicating that only the weakly bound OTf^- ligand of Cr in **3** was replaced by NCS^-. The Cr−NCS distance of 2.22 Å is only somewhat shorter than in the NCS adduct of dichromium tetrakispropionate (2.25 Å).[12] The Cr−N−C angle of 179° may indicate that the NCS ligand is also acting as a π donor in this compound, though the Cr≡Cr bond length of 2.02 Å remains short.

Compound **5** was crystallized as **5**·$0.5CH_2Cl_2$·0.15THF from CH_2Cl_2/hexanes (Figure 4). The crystal structure contains two molecules of **5** in the asymmetric unit. The metal atoms of each independent molecule are disordered with relative occupancies of 76%/24% for one molecule, and 57%/43% for the other molecule. The metal−ligand and metal−metal distances in these four distinct molecules span an unusually broad range: Fe−O, Cr···Fe, and Cr−Cr distances vary from 1.95 to 2.10 Å, 2.59 to 2.74 Å, and 1.84 to 2.01 Å, respectively. It is not clear at this point what causes these remarkable structural variations in the solid state, though the metal atom positions of the 24% occupied orientations are most likely inaccurate. We note that ^{1}H NMR experiments (*vide infra*) show the presence of only one species in solution.

2. Assignment of the Noncentrosymmetric Space Group Cc. The structures of compounds **3**, **4**, **5**, and **8**/**8-iso** were all solved in the space group *Cc*, which is a somewhat problematic space group because its systematic absences also fit the centrosymmetric space group *C*2/*c*. Intensity statistics for the X-ray data can be inconclusive; thus, a discussion of the choice of space

dx.doi.org/10.1021/ic2011309 |*Inorg. Chem.* 2011, 50, 10592–10599

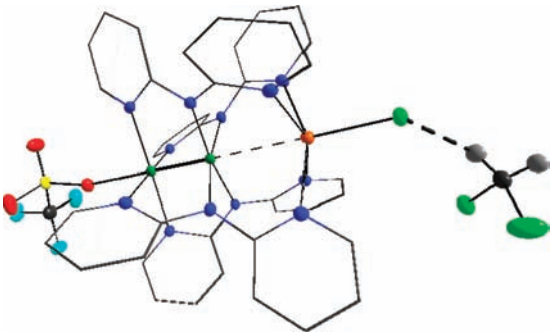

Figure 3. Molecular structure of **4** highlighting the intermolecular Mn−Cl···H(CH_2Cl_2) interaction on the right (Cr: dark green, Mn: orange, Cl: green, N: blue, F: light blue, O: red).

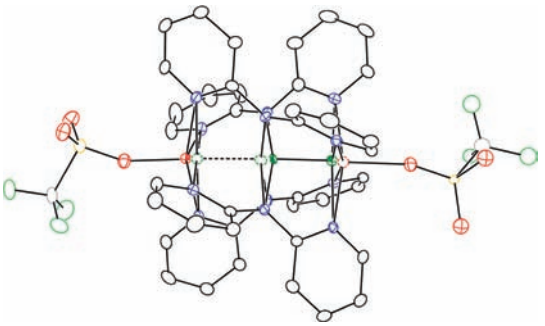

Figure 4. Molecular structure of one of the two independent trinuclear molecules in **5**·0.5CH_2Cl_2·0.3C_4H_8O showing the Fe (red) and Cr (green) disorder, with displacement ellipsoids drawn at the 30% probability level. Hydrogen atoms have been omitted for clarity.

group and refinement is warranted. For compounds **3**, **4** and **8**/**8-iso**, the statistics favor a noncentrosymmetric structure, indicating that the *Cc* space group provides a better fit for the data. Deeper inquiry reveals the structures to be pseudosymmetric and, in all cases, the triflate moiety breaks the center of symmetry. The refinement in *Cc*, however, is not straightforward, since **3**, **4**, and **8**/**8-iso** refine with Flack parameter[13] values of 0.495(13), 0.50(11), and 0.54(13), respectively, suggesting that the centrosymmetric structure may indeed be correct. Our best attempts to refine these structures in *C*2/*c* with disordered triflates led to unstable refinements with wR2 values of 0.4038, 0.4201, 0.3491, and 0.4691 for **3**, **4**, **5**, and **8**/**8-iso**, respectively, which we deemed unacceptable. The only structure solution for each of these data sets that produced chemically reasonable and computationally stable refinements was a refinement in space group *Cc* as a racemic twin.

Using similar methods, compound **5** was found to be a racemic twin with a minor component contribution of 0.19(3). Attempts to refine the structure in the centrosymmetric space group *C*2/*c* were unfruitful and were not computationally stable. In addition, inspection of the correlation matrices for these structures does not reveal any correlation between would-be symmetry-related parameters, which is a strong indication that the structure is not centrosymmetric. The identities of important atoms such as the metal centers were consistent with structures of the dichloro precursor molecules.

3. Structural Changes Induced by Ligand Substitution. Regiospecific substitution of the chromium bound Cl_{Cr} of **1** and **2** by OTf^- in **3** and **4** or NCS^- in **6** causes a variety of structural changes. As one would anticipate from the substantial work previously done on Cr≡Cr bonded compounds,[14] changing the Cr axial ligand has a meaningful effect on the Cr≡Cr bond distance[15] and, to a lesser extent, the outer Cr−N bond distances. Specifically, the Cr≡Cr bond distance decreases in length from 2.025(2) to 2.0187(8) to 1.9641(7) Å as the axial ligand is changed from chloride (**1**) to thiocyanate (**6**) to triflate (**3**). The shortening of the metal−metal bond distance is accompanied by a concomitant decrease in the equatorial Cr_{outer}−N distances of ∼0.05 Å. The Cr≡Cr and Cr_{outer}−N distances of the manganese analogs shorten consistently from 2.040(1) to 1.9573(6) Å (by ∼0.08 Å) and from 2.130[5] to 2.076[3] Å (by ∼0.05 Å), respectively, upon substituting Cl_{Cr} by OTf.

Although the interrelatedness of Cr−Cr, Cr−axial ligand, and Cr−equatorial ligand bonding has been established,[14] the different Cr axial ligands also remotely and unexpectedly influence the geometry of the Fe or Mn center. As the Cr_{outer}−N bond distances become shorter, the Fe−N and Mn−N bond distances uniformly become longer by as much as 0.04 Å and 0.07 Å, respectively, in a more or less linear relationship. The changes in the Fe−N and Mn−N bond distances may be described as a teeter-totter-like "tilting" of the ligand about its central Cr−N bond. Thus, the identity of the Cr axial ligand may be used here to tune the ligand field of the Fe or Mn atoms in these compounds.

We may define a "degree of tilting" (δ) of the dpa ligand in these compounds as $\delta = d(M-N) - d(Cr-N_{outer})$ with M = Mn, Fe or Co. From the δ values listed in Table 2, we can see a clear correlation with Cr≡Cr bond distances, stemming from the established direct relationship between Cr−equatorial ligand bond distance and Cr≡Cr bond distance. Notably, there is no correlation between values of δ and the heterometallic Cr···M separations. We have recently provided evidence that the magnetic anisotropy of M is affected by the quadruple bond,[4] but it is important to point out here that no relationship between the heterometallic separations and any of the geometric features of M is apparent, although the axial M−Cl distances are, in certain cases, obscured by an intermolecular interaction with a solvent molecule. Further, although it would be useful to quantify the magnitude of the "tilting" effect on the ligand field of M by probing the metal ligand field transitions with UV−vis spectroscopy, the Fe ligand field transitions have not been observable in these compounds and Mn(II) does not have spin-allowed bands.

Additionally, the axial Fe−Cl and Mn−Cl distances elongate by 0.09 and 0.11 Å in going from **1** and **2** to **3** and **4**, respectively. This elongation is presumably due to some extent to the above-mentioned interaction between the axial Cl^- and a CH_2Cl_2 solvent molecule and it is therefore somewhat ambiguous in these compounds as to whether the change is due to the exchange of Cr axial ligands. However, the Fe−Cl bond in **6** is not perturbed by any intermolecular interactions, and its elongation by ∼0.05 Å as compared to **1** is therefore a clear result of the remote effect of substituting Cl^- for NCS^- at Cr.

Similar structural changes are observed for the N_4CoCl unit in compound **8** although structural comparison to the dichloro compound **7** is complicated by the temperature-dependence of the spin-state of the Co(II) ion in **7**. It has been shown by variable temperature (VT) magnetic susceptibility and VT crystallography that the Co(II) ion in **7** is low-spin (S = 1/2) at low temperature (∼100 K) and high-spin (S = 3/2) at room temperature.[6] The Co−N and Co−Cl distances (at 100 K) in **8** of 2.161[5] Å and 2.359(2) Å, respectively, are indicative of

dx.doi.org/10.1021/ic2011309 |*Inorg. Chem.* 2011, 50, 10592–10599

Table 3. ^{1}H NMR Resonances (ppm) in 1, 3, 5, and 6 and Their Assignments

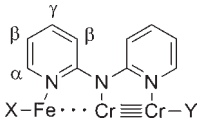

compound	α	β	γ	Cr bound pyridine protons
1	107.35	68.26	−5.54	6.36, 5.61, 3.21, 1.86
X = Y = Cl		39.36		
3	112.36	70.66	−1.97	6.39, 4.30, 4.09, 3.64
X = Cl, Y = OTf		40.49		
5	105.02	71.23	−2.65	4.49, 3.84, 2.47, −0.76
X = Y = OTf		39.29		
6	108.06	69.08	−4.51	5.92, 4.90, 2.88, 1.52
X = Cl, Y = SCN		39.27		

high-spin Co(II) and can be compared to the room temperature structure of **7**, having shorter Co−N distances of 2.125[3] Å and a rather long Co−Cl bond length of 2.370(1) Å. Thus, the "tilting" of the dpa ligand away from Co is also observed in going from **7** to **8** and, more importantly, the tilt of the dpa ligand in **8** causes the Co(II) ion to remain high-spin at 100 K, whereas the Co(II) ion in **7** is mostly low-spin at this temperature. This effect is a clear indication of a weaker ligand field being exerted in **8** than in **7**.

The N_4CoOTf unit in **8-iso** has short Co−N distances of 2.03[2] Å, which are indicative of low-spin Co(II) and similar to the Co−N bond lengths in the low-spin form of **7** (2.054(2) Å). The axial Co−O distance of 2.18(1) Å in **8-iso** is shorter than the Co−OSO_2CF_3 bond lengths of 2.244(3) Å and 2.223(3) Å in the homometallic pentanuclear ditriflate compound $Co_5(tpda)_4(OTf)_2$ (tpda = the dianion of *N*,*N*-bis(α-pyridyl)-2,6-diaminopyridine)[16] and the hexanuclear $[Co_6(\mu_6\text{-bpyany})_4(OTf)_2](OTf)_2$ (bpyany = dianion of 2,7-bis(a-pyridylamino)-1,8-naphthyridine),[17] respectively. It is remarkable that the substitution of the stronger σ donor chloro ligand by the weaker OTf^- ligand at Co causes the Co(II) ion in **8-iso** to be low-spin at 100 K, but this is likely due to the lesser π-donation of triflate as compared to chloride. The presence of two Co ions of different spin states in the **8**/**8-iso** mixture in frozen solution was also evidenced by EPR spectroscopy (*vide infra*).

^{1}H NMR and EPR Spectroscopy. The Fe-ligand bond distances in **1**, **3**, **5**, and **6** are all suggestive of a high-spin Fe(II) ion with an $S = 2$ magnetic ground state. This ground state assignment has been verified by room-temperature magnetic susceptibility measurements on **1**, **3**, and **5**. Despite their paramagnetism, ^{1}H NMR spectra could be measured for these Fe(II) compounds. ^{1}H NMR spectra of the paramagnetic compounds **1**, **3**, **5**, and **6** in CD_2Cl_2 display eight well-resolved signals in the range of 115 to −6 ppm (Table 3). The peaks corresponding to the protons of the Fe-bound pyridine moiety of the dpa ligand were assigned considering the characteristic ^{1}H NMR signal pattern of iron/pyridine complexes.[18] These signals show a remarkable sensitivity to Cl_{Cr} substitution for OTf^- and SCN^- in going from **1** to **3** and **3** to **6**, respectively. The chemical shift of the Cr-bound pyridine protons in **1**, **3**, and **6** are less affected by the paramagnetism in that they appear at a more intuitive, "diamagnetic" region of the ^{1}H NMR spectrum. However, in **5** we find these proton resonances to be significantly shifted upfield

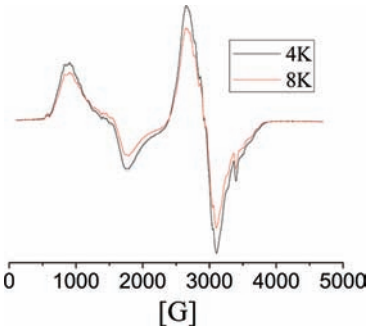

Figure 5. X-band EPR spectrum of a frozen solution (CH_2Cl_2) of the **8**/**8-iso** mixture.

and note that the chemical shifts of the individual Cr-bound pyridine protons vary more than what would be expected based on the diamagnetic anisotropy of the quadruple bond.[14,19] Most importantly, compound **3** shows only one set of ^{1}H NMR signals, verifying that it is a pure compound and that **3-iso** is not present. Also, the proposed altered bonding of the dpa ligand upon regioselective ligand substitution in going from **1** to **3** and **3** to **6**, as deduced from the solid state crystallographic results above, appears to be present in solution as well, as all the Fe-pyridine NMR signals shift monotonically from **1** to **6** to **3**.

The ^{1}H NMR spectrum of the paramagnetic compound **8**/**8-iso** CD_2Cl_2 displays many signals in the range of 120 to −10 ppm, indicating the presence of two compounds, a major product and minor product. Accurate integrations of these signals were inaccessible due to broadening of the signals. The peaks corresponding to the protons of the Co-bound pyridine moiety of the dpa ligand of the major product appear at α = 117.86 ppm, β = 49.45 and 74.57 ppm, and the minor product at α = 108.24 ppm, β = 46.37 and 68.76 ppm. The γ protons were obscured by resonances from the other pyridine ring and could not be assigned unambiguously. The positions of these peaks are markedly similar to those of compound **3** and are therefore assigned analogously. It is remarkable that the pyridine resonances for both **8** and **8-iso** appear in a range similar to each other. Due to the two different spin states of **8** and **8-iso** suggested by the crystal structure, one might expect high-spin and low-spin resonances to occur in significantly different chemical shift ranges. Instead, this is not observed and the peak positions suggest that at room temperature in solution, both **8** and **8-iso** are high spin. The chemical shifts of the Cr-bound pyridine protons of the major and minor products are difficult to distinguish because of the broadening of the signals caused by paramagnetism, although they fall in range from −8 to 8 ppm, which is a similar, albeit larger, range compared to that of compounds **1**, **3**, **5**, and **6**.

The 4 K X-band EPR spectrum of a frozen solution of the **8**/**8-iso** mixture in CH_2Cl_2 (Figure 5) displays one signal at g_{obs} = 4.81 and one more intense signal at g_{obs} = 2.29. The major signal is clearly due to a slightly axial $S = 1/2$ system, and the g value of 2.29 is in good agreement with low-spin Co(II) (indicative of **8-iso**) since the more than half-filled set of d orbitals gives rise to g values greater than 2. The g = 4.8 signal is assigned to a Co(II) high-spin ($S = 3/2$) ion in **8**. This assignment is made based on similar assignments for the corresponding Mn(II) compounds.[4] In the case of the Co(II) and Mn(II) compounds, the axial zero-field splitting parameter D is larger than the microwave quantum and therefore, effective g values of 6 for the $S = 5/2$ state and 4 for the $S = 3/2$ state are expected from rhombograms for the fully

dx.doi.org/10.1021/ic2011309 |*Inorg. Chem.* 2011, 50, 10592–10599

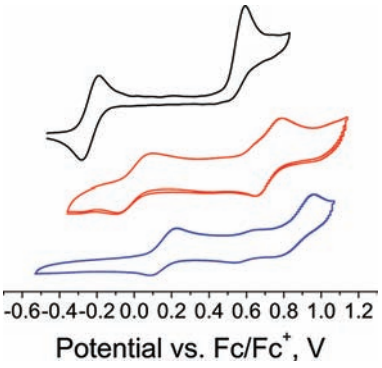

Figure 6. Cyclic voltammogram of **1** (top), **3** (middle), and **5** (bottom) in CH_2Cl_2.

axial case (E/D = 0). The splitting of the $g = 4$ signal of **8** is consistent with a deviation from true axial symmetry, roughly to E/D ~ 0.12.

Electrochemistry. We also investigated how the Cr axial ligand exchange affects the redox properties of Fe in **3** (Figure 6). The cyclic voltammogram (CV) of **1** in CH_2Cl_2 exhibits a reversible iron centered oxidation wave at −236 mV and an irreversible wave at 538 mV.[5] The dominant features of the cyclic voltammogram of **3** are two oxidation waves, which appear both quasireversible and of the same peak height. The first oxidation wave is observed at −4 mV and the second is observed at 720 mV (potentials referenced vs Fc/Fc^+). The first oxidation event in **3** is proposed to be the $Fe^{2+/3+}$ redox couple of the N_4FeCl unit in analogy to the redox properties of **1**. The shift to higher potential is likely due to both the lesser electron donating ability of OTf^- in **3** as compared to **1** and the longer Fe−dpa bond distances (weaker ligand field), which renders the Fe^{2+} ion in **3** more difficult to oxidize as compared to **1**. The second oxidation wave in the CV of **3** shows reversible features and may be ascribed to either the $Cr_2^{4+/5+}$ or the $Fe^{3+/4+}$ redox couple. The CV of the ditriflate compound **5** displays one nonreversible oxidation at 156 mV and further oxidation events at even higher potential.

Summary. Substitution of the axial chloride ligand in **1** and **2** with OTf^- occurs regiospecifically at Cr yielding the monotriflate compounds **3** and **4**. For **7** no such selectivity was found. Most importantly, we found that the environment of the heterometal Fe, Mn, or Co can be altered without changing its primary coordination sphere. In detail, the introduction of a weaker axial ligand (OTf) to the Cr_2 unit causes a physical tilting of the dpa ligand toward its Cr_2-bound region, thereby weakening its binding to Fe, Mn, or Co. This effect significantly alters the ligand field strength and the redox properties of Fe(II) in the CrCrFe chains, elongates the axial Fe−Cl bond, and makes the Fe more difficult to oxidize.

■ ASSOCIATED CONTENT

Supporting Information. Figure S1 and crystallographic data in CIF format. This material is available free of charge via the Internet at http://pubs.acs.org.

■ AUTHOR INFORMATION

Corresponding Author
*E-mail: berry@chem.wisc.edu.

■ ACKNOWLEDGMENT

We thank the National Science Foundation for support under CHE-0745500.

■ REFERENCES

(1) (a) Berry, J. F. In *Structural Bonding (Berlin)*, Vol. 136; Mingos, D. M. P., series Ed.; Parkin, G., volume Ed.; Springer-Verlag: Berlin, 2010. (b) Meng, X.; Wang, F. S.; Jin, G. X. *Coord. Chem. Rev.* **2010**, *254*, 1260. (c) Diaconescu, P. L. *Acc. Chem. Res.* **2010**, *43*, 1352. (d) Diaconescu, P. L. *Comments Inorg. Chem.* **2010**, *31*, 196. (e) Marinescu, G.; Andruh, M.; Lloret, F.; Julve, M. *Coord. Chem. Rev.* **2011**, *255*, 161. (f) Mandal, S. K.; Roesky, H. W. *Acc. Chem. Res.* **2010**, *43*, 248.

(2) (a) Sculfort, S.; Welter, R.; Braunstein, P. *Inorg. Chem.* **2010**, *49*, 2372. (b) Navulla, A.; Tsirlin, A. A.; Abakumov, A. M.; Shpanchenko, R. V.; Zhang, H. T.; Dikarev, E. V. *J. Am. Chem. Soc.* **2011**, *133*, 692. (c) Li, B.; Zhang, H. T.; Huynh, L.; Diverchy, C.; Hermans, S.; Devillers, M.; Dikarev, E. V. *Inorg. Chem.* **2009**, *48*, 6152. (d) Dikarev, E. V.; Li, B.; Rogachev, A. Y.; Zhang, H. T.; Petrukhina, M. A. *Organometallics* **2008**, *27*, 3728. (e) Dikarev, E. V.; Li, B.; Zhang, H. T. *J. Am. Chem. Soc.* **2006**, *128*, 2814. (f) Bruce, M. I.; Humphrey, P. A.; Zaitseva, N. N.; Nicholson, B. K.; Skelton, B. W.; White, A. H. *Dalton Trans.* **2010**, *39*, 8801. (g) Colson, A. C.; Whitmire, K. H. *Organometallics* **2010**, *29*, 4611. (h) Stavila, V.; Thurston, J. H.; Whitmire, K. H. *Inorg. Chem.* **2009**, *48*, 6945. (i) Ould-Ely, T.; Thurston, J. H.; Whitmire, K. H. *C. R. Chim.* **2005**, *8*, 1906. (j) Huang, W.; Carver, C. T.; Diaconescu, P. L. *Inorg. Chem.* **2011**, *50*, 978. (k) Cooper, B. G.; Fafard, C. M.; Foxman, B. M.; Thomas, C. M. *Organometallics* **2010**, *29*, 5179. (l) Thomas, C. M.; Napoline, J. W.; Rowe, G. T.; Foxman, B. M. *Chem. Commun.* **2010**, *46*, 5790. (m) Greenwood, B. P.; Forman, S. I.; Rowe, G. T.; Chen, C. H.; Foxman, B. M.; Thomas, C. M. *Inorg. Chem.* **2009**, *48*, 6251. (n) Rampersad, M. V.; Zuidema, E.; Ernsting, J. M.; van Leeuwen, P.; Darensbourg, M. Y. *Organometallics* **2007**, *26*, 783. (o) Zhou, W.; Napoline, J. W.; Thomas, C. M. *Eur. J. Inorg. Chem.* **2011**, 2029.

(3) (a) Huang, D. G.; Holm, R. H. *J. Am. Chem. Soc.* **2010**, *132*, 4693. (b) Groysman, S.; Majumdar, A.; Zheng, S. L.; Holm, R. H. *Inorg. Chem.* **2010**, *49*, 1082. (c) Hlavinka, M. L.; Miyaji, T.; Staples, R. J.; Holm, R. H. *Inorg. Chem.* **2007**, *46*, 9192. (d) Sun, J. B.; Tessier, C.; Holm, R. H. *Inorg. Chem.* **2007**, *46*, 2691. (e) Pesavento, R. P.; Berlinguette, C. P.; Holm, R. H. *Inorg. Chem.* **2007**, *46*, 510. (f) Berlinguette, C. P.; Holm, R. H. *J. Am. Chem. Soc.* **2006**, *128*, 11993. (g) Osterloh, F.; Achim, C.; Holm, R. H. *Inorg. Chem.* **2001**, *40*, 224. (h) Osterloh, F.; Segal, B. M.; Achim, C.; Holm, R. H. *Inorg. Chem.* **2000**, *39*, 980. (i) Osterloh, F.; Sanakis, Y.; Staples, R. J.; Münck, E.; Holm, R. H. *Angew. Chem., Int. Ed.* **1999**, *38*, 2066. (j) Darensbourg, M. Y.; Weigand, W. *Eur. J. Inorg. Chem.* **2011**, 994. (k) Almaraz, E.; Foley, W. S.; Denny, J. A.; Reibenspies, J. H.; Golden, M. L.; Darensbourg, M. Y. *Inorg. Chem.* **2009**, *48*, 5288. (l) Barton, B. E.; Whaley, C. M.; Rauchfuss, T. B.; Gray, D. L. *J. Am. Chem. Soc.* **2009**, *131*, 6942. (m) Barton, B. E.; Rauchfuss, T. B. *J. Am. Chem. Soc.* **2010**, *132*, 14877. (n) Nayak, S.; Pada, H.; Dehnen, S.; Powell, A. K.; Reedjik, J. *Dalton Trans.* **2011**, 2699. (o) Mishra, A.; Yano, J.; Pushkar, Y.; Yachandra, V. K.; Abboud, K. A.; Christou, G. *Chem. Commun.* **2007**, 1538. (p) Ogo, S.; Kabe, R.; Uehara, K.; Kure, B.; Nishimura, T.; Menon, S. C.; Harada, R.; Fukuzumi, S.; Higuchi, Y.; Ohhara, T.; Tamada, T.; Kuroki, R. *Science* **2007**, *316*, 585. (q) Kure, B.; Ogo, S.; Inoki, D.; Nakai, H.; Isobe, K.; Fukuzumi, S. *J. Am. Chem. Soc.* **2005**, *127*, 14366. (r) Ogo, S.; Suzuki, T.; Ozawa, Y.; Isobe, K. *Inorg. Chem.* **1996**, *35*, 6093.

(4) Nippe, M.; Wang, J.; Bill, E.; Hope, H.; Dalal, N. S.; Berry, J. F. *J. Am. Chem. Soc.* **2010**, *132*, 14261.

(5) Nippe, M.; Berry, J. F. *J. Am. Chem. Soc.* **2007**, *129*, 12684.

(6) Nippe, M.; Victor, E.; Berry, J. F. *Eur. J. Inorg. Chem.* **2008**, *2008*, 5569.

(7) Nippe, M.; Bill, E.; Berry, J. F. *Inorg. Chem.* **2011**, *50*, 7650.

(8) Bain, G.; Berry, J. F. *J. Chem. Educ.* **2008**, *85*, 532.

(9) *APEX2, SADABS, and SAINT Software Reference Manuals*; Bruker-AXS: Madison, WI, USA, 2009.

(10) Dolomanov, O. V.; Bourhis, L. J.; Gildea, R. J.; Howard, J. A. K.; Puschmann, H. *J. Appl. Crystallogr.* **2009**, *42*, 339.
(11) Spek, A. L. *J. Appl. Crystallogr.* **2003**, *36*, 7.
(12) Ford, P. D.; Larkworthy, L. F.; Povey, D. C.; Roberts, A. J. *Polyhedron* **1983**, *2*, 1317.
(13) Flack, H. D. *Acta Crystallogr.* **1983**, *A39*, 876.
(14) Cotton, F. A. In *Multiple Bonds Between Metal Atoms*, 3rd ed.; Cotton, F. A., Murillo, C. A., Walton, R. A., Eds.; Springer Science and Business Media: New York, 2005.
(15) The nature of the Cr−Cr multiple bond is defined by the distribution of states of different configurations with different populations of bonding and antibonding molecular orbitals; e.g., $\sigma^2\pi^4\delta^2$, $\sigma^2\pi^4\delta^1\delta^{*1}$,... . The length of the Cr≡Cr quadruple bond is generally regarded to be highly affected by the extent to which an axial ligand modifies electron density in the antibonding orbitals of this multiple bond.
(16) Yeh, C.-Y.; Chou, C.-H.; Pan, K.-C.; Wang, C.-C.; Lee, G.-H.; Su, Y. O.; Peng, S.-M. *J. Chem. Soc., Dalton Trans.* **2002**, 2670.
(17) Chien, C.-H.; Chang, J.-C.; Yeh, C.-Y.; Lee, G.-H.; Fanga, J.-M.; Peng, S.-M. *J. Chem. Soc., Dalton Trans.* **2006**, 2106.
(18) (a) Klinker, E. J.; Kaizer, J.; Brennessel, W. W.; Woodrum, N. L.; Cramer, C. J.; Que, L., Jr. *Angew. Chem., Int. Ed.* **2005**, *44*, 3690. (b) Zang, Y.; Kim, J.; Dong, Y. H.; Wilkinson, E. C.; Appelman, E. H.; Que, L., Jr. *J. Am. Chem. Soc.* **1997**, *119*, 4197.
(19) (a) Collman, J. P.; Barnes, C. E.; Swepston, P. N.; Ibers, J. A. *J. Am. Chem. Soc.* **1984**, *106*, 3500. (b) Collman, J. P.; Garner, J. M.; Hembre, R. T.; Ha, Y. *J. Am. Chem. Soc.* **1992**, *114*, 1292.